Article published online: 2021-07-30

Thumb ultrasound: Technique and pathologies

Jatinder P Singh, Shwetam Kumar, Atman V Kathiria, Rachit Harjai, Akram Jawed[1], Vikas Gupta[1]

Department of Imaging and Nuclear Medicine and [1]Bone and Joint Institute, Medanta, The Medicity, Gurgaon, Haryana, India

Correspondence: Dr. Jatinder P Singh, Senior Consultant Radiologist, Medanta, The Medicity, Gurgaon, Haryana, India.
E-mail: jatinder.singh@medanta.org

Abstract

Ultrasound is ideally suited for the assessment of complex anatomy and pathologies of the thumb. Focused and dynamic thumb ultrasound can provide a rapid real-time diagnosis and can be used for guided treatment in certain clinical situations. We present a simplified approach to scanning technique for thumb-related pathologies and illustrate a spectrum of common and uncommon pathologies encountered.

Key words: Pathology; technique; thumb; ultrasound

Introduction

The intricate anatomy of the thumb has evolved over millions of years and allows us to perform delicate precision tasks and gives a powerful grip to the hand. Accurately scanning the thumb can be challenging and time consuming for a beginner due to its relatively small size and complex anatomy. There are many situations where ultrasound is found to be a superior imaging investigation than magnetic resonance imaging (MRI) because of its dynamic nature, better resolution for smaller structures, low cost, and because it is easy and quick to use in trained hands. We present a simplified approach to scanning technique for thumb-related pathologies and illustrate a spectrum of common and uncommon pathologies encountered.

Videos Available on: www.ijri.org

Access this article online	
Quick Response Code:	Website: www.ijri.org
	DOI: 10.4103/0971-3026.190408

Technique and Pathologies

The standard ultrasound examination of the thumb begins with the patient sitting in front of the examiner with their hand on a pillow. Good-quality ultrasound equipment and a high-frequency (12–15 MHz) linear-array (with a flat surface) probe is required. A dedicated smaller and convenient hockey stick probe can also be used, especially to assess ulnar collateral ligament. The probe should be held at its end with the edge of the hand resting on the pillow in order to reduce stress and allow fine motor control. A gel stand should be used to improve visualization by reducing pressure on soft structures. Obtaining a brief history at the beginning of the examination can provide clues to the underlying pathology. The evaluation of the problem pertaining to the thumb should include evaluation of the thumb, radial

Cite this article as: Singh JP, Kumar S, Kathiria AV, Harjai R, Jawed A, Gupta V. Thumb ultrasound: Technique and pathologies. Indian J Radiol Imaging 2016;26:386-96.

aspect of the wrist, and the forearm because the muscles and tendons of the thumb originate in the forearm and traverse the wrist to reach the thumb. Various nerve and vascular pathologies at the level of the wrist and the forearm can also produce symptoms pertaining to the thumb, and these should also be evaluated.

Evaluation of bones and joints

Bony pathologies such as cortical breach, bony processes, or scalloping are usually detected while evaluating soft tissue structures. Ultrasound may be useful in detecting fractures, which appear as focal cortical break of the hyperechoic cortical line, usually associated with periosteal thickening and subperiosteal hematoma.

Important joints to be evaluated are interphalangeal, first carpometacarpal (CMC)/trapeziometacarpal joint and scaphotrapeziotrapezoid (STT) joint. The first CMC joint is best examined with the patient seated opposite and placing the ulnar aspect of their hand against the examination couch—karate chop position [Figure 1A] with the probe placed in the sagittal plane. The first metacarpal is distinguished from the much shorter trapezium and, from this landmark, the CMC joint is easily found [Figure 1B]. Scaphotrapeziotrapezoid joint can be evaluated by moving the probe proximally in the sagittal plane [Figure 1C]. Then we have the metacarpophalengeal and interphalengeal joint, which can be evaluated while assessing the extensor and flexor tendons [Figure 1D-K].

These joints are evaluated for any effusion, synovial thickening, erosions, osteophytes, articular cartilage defect, bony avulsion, or alignment abnormality. Joint effusion and synovial proliferation can be seen in inflammatory arthritis, degenerative joint disease (DJD), or infective arthritis. Synovitis is usually more echogenic and exhibits Doppler signal in the active phase [Figure 2A]. Joint effusion is hypoechoic, avascular, and expelled from the joint recess with transducer compression [Figure 2B and C]. Erosions [Figure 2D] are noted in inflammatory arthritis whereas osteophytes are more specific for DJD. Ultrasound and plain radiographs help in staging of DJD, which gives rationale for treatment.[1] Ultrasound features of infective arthritis include synovitis, effusion, and subperiosteal collection with the final diagnosis by ultrasound-guided diagnostic joint aspiration.

Evaluation of tendons

Flexor pollicis longus (FPL) is seen on the palmar surface of the wrist and can be located at two levels in the transverse probe position at proximal and distal carpal tunnel by locating scaphoid tubercle and pisiform (proximal level) and

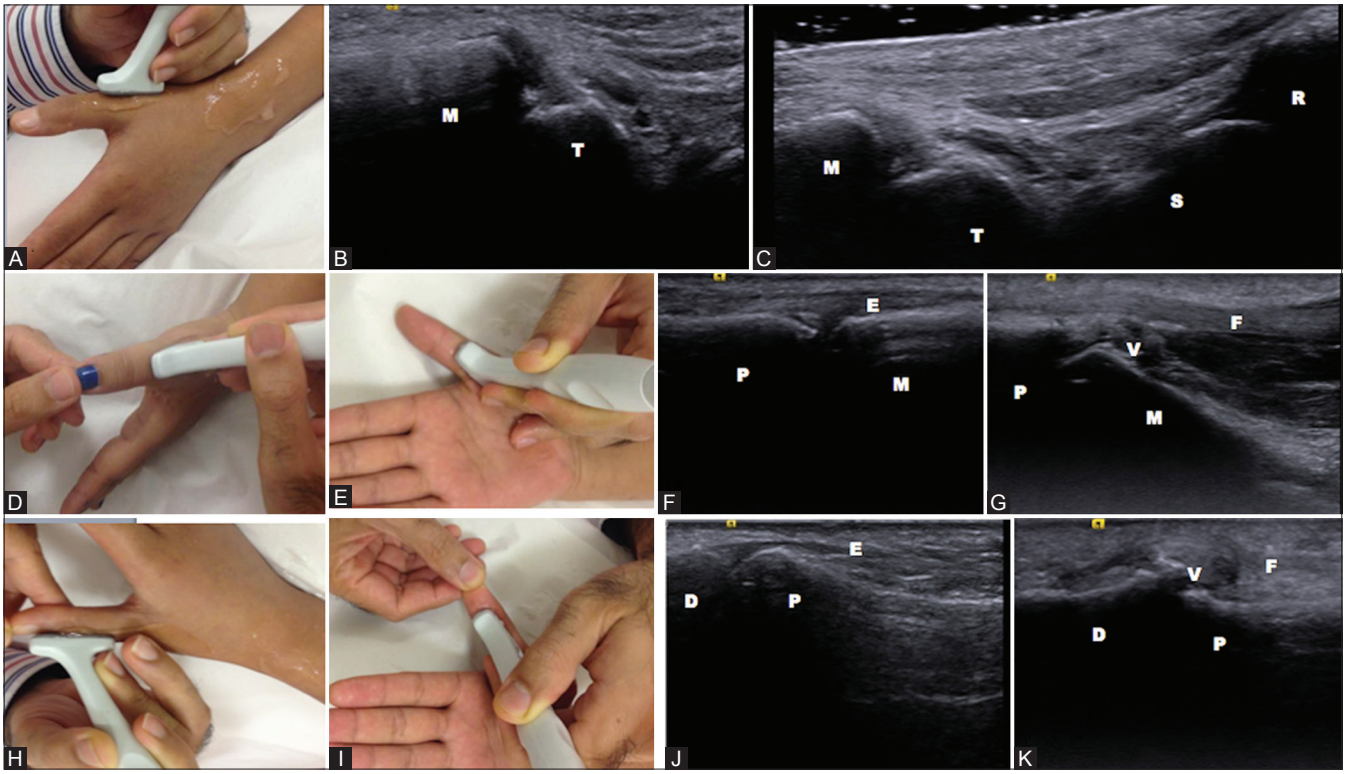

Figure 1 (A-K): Probe positions and ultrasound images for evaluation of joints (A-K). Karate chop position of the hand with probe (A) and corresponding ultrasound image of the carpometacarpal joint (B). Ultrasound image of STT joint (C). Probe position for metacarpophalengeal joint, dorsal (D) and volar (E) with corresponding ultrasound image (F and G). Probe position for interphalengeal joint, dorsal (H), and volar (I) with corresponding ultrasound image (J and K). (Radius - R, scaphoid - S, 1st metacarpal - M, trapezium - T, proximal phalynx - P, distal phalynx - D, FPL - F, volar/palmar plate – V, and EPL - E.)

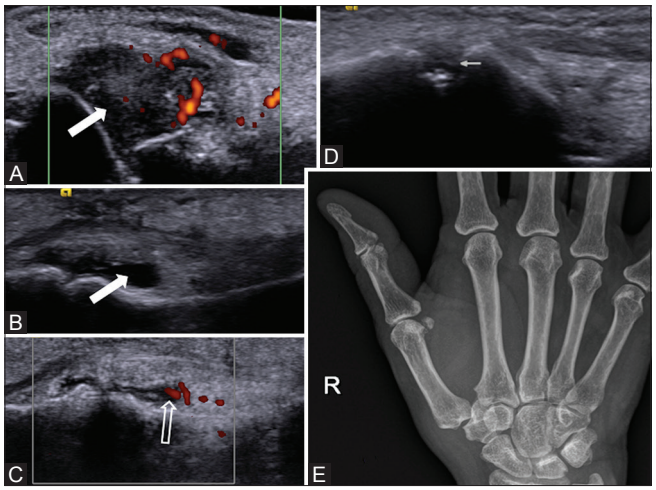

Figure 2 (A-E): Inflammatory arthritis of the thumb in a HLA-B27 positive patient (A-E). Long axis (A) ultrasound view of the first carpometacarpal joint shows synovial thickening (arrow) with increased vascularity on Doppler. Long axis ultrasound images of the volar aspect of metacarpophalengeal joint without (B) and with pressure (C) shows displaced joint fluid (arrow in B) and minimal synovium with increased vascularity (open arrow in C). Long axis ultrasound view of the metacarpophalengeal joint (D) shows periarticular erosion (small arrow). Antero-posterior radiograph (E) of the same patient does not reveal any abnormality

trapezium and hook of hamate (distal level). FPL tendon is seen just medial to the scaphoid tubercle and trapezium. The FPL is then evaluated in the thenar eminence in long and short axis with the hand in supinated position [Figure 3A-D] along with the thenar muscles. Moving the thumb can be helpful in identifying the tendon.

The extensor tendons of the thumb are situated in the 1st (abductor pollicis longus and extensor pollicis brevis - APL and EPB) and 3rd (extensor pollicis longus - EPL) extensor compartments on the dorsal aspect of the wrist. These tendons should be first located and then traced proximally up to the myotendinous junction and distally to their insertion. To identify the extensor tendons locate Lister's tubercle [Figure 3E-G] on the dorsal aspect of the wrist, the tendon in its medial aspect is EPL (3rd extensor compartment) and the tendons in its lateral aspect are extensor carpi radialis longus and brevis (2nd extensor compartment) and APL and EPB (1st extensor compartment) [Figure 3H and I]. After slight supination of the hand (karate chop position), the 1st extensor compartment tendons are traced proximally, where they cross over the 2nd compartment muscles (proximal intersection point)

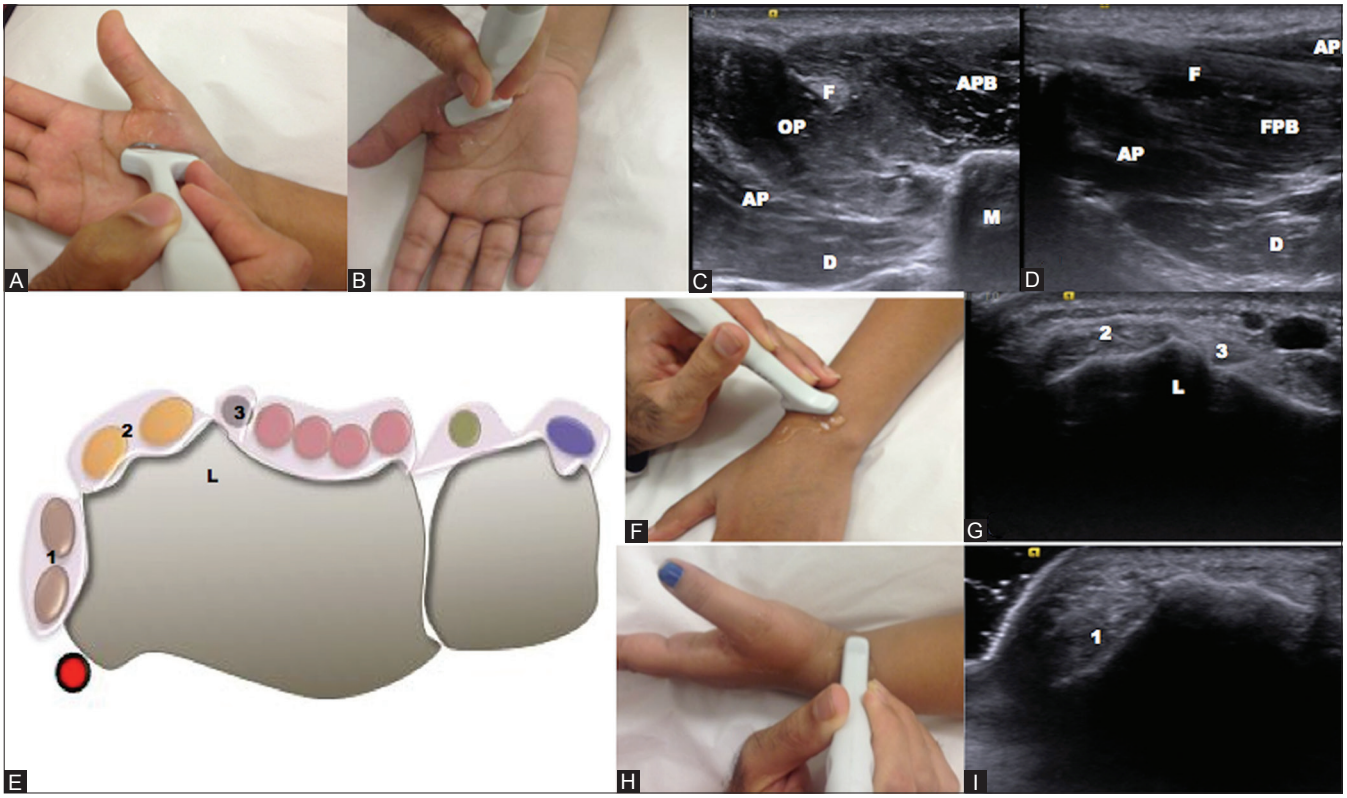

Figure 3 (A-I): Probe positions and ultrasound for evaluation of thenar muscles, FPL and extensor compartment tendons of the thumb (A-I). Probe position in short (A) and long (B) axis with corresponding ultrasound image (C and D) of thenar muscles and the flexor pollicis longus. Schematic diagram (E), probe position (F), and ultrasound image (G) shows Lister's tubercle, EPL and 2nd compartment tendons. Probe position (H) and ultrasound image (I) shows the 1st compartment tendons. (FPL- F, metacarpal - M, dorsal interossei – D, Lister's Tubercle - L, 1st compartment - 1, 2nd compartment - 2, 3rd compartment tendons - 3)

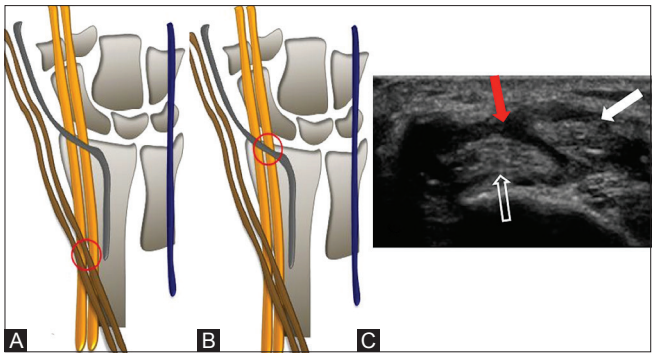

Figure 4 (A-C): Proximal and distal intersection points with distal intersection syndrome (A-C). Schematic diagram (A) shows the 1st extensor compartment tendons (brown) crossing over the 2nd extensor compartment tendons (yellow)—proximal intersection point (red circle). Schematic diagram (B) shows the extensor pollicis longus (EPL) tendon (grey) crossing over 2nd extensor compartment tendons (yellow) - distal intersection point (red circle). Short axis (C) ultrasound showing the tendon (white arrow) crossing over the 2nd extensor compartment tendons (open arrow) associated with tendon sheath thickening (red arrow)

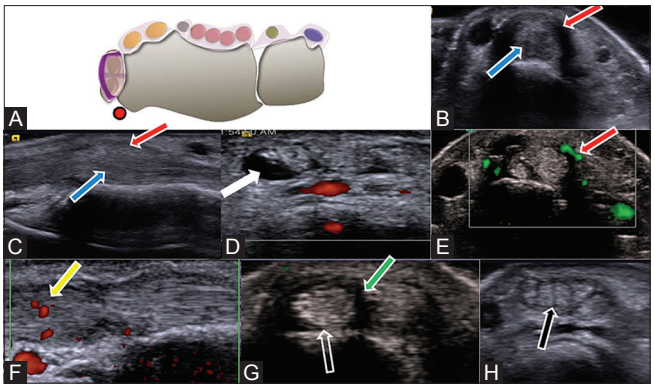

Figure 5 (A-H): De Quervain's tenosynovitis (A-H). Schematic diagram (A) shows thickened extensor retinaculum (in purple) around the 1st extensor tendons. Short (B) and long axis (C) ultrasound show thickened extensor retinaculum (red arrow) with swollen 1st compartment tendons (blue arrow). Short axis ultrasound images show peritendinous fluid (white arrow) (E), increased retinaculum vascularity (red arrow) (F), intratendinous Doppler flow (yellow arrow) (G), isolated EPB tendon involvement (open arrow) with septa (green arrow) and multiple 1st extensor compartment tendon slips (black arrow)

[Figure 4A]. The EPL (3rd compartment) tendon is traced distally, where it crosses 2nd extensor compartment tendons (distal intersection point) [Figure 4B]. Because of the mechanical friction at the level of these crossings, changes of tendinosis, peritendinous edema with loss of intervening fat and tendon tear can occur, which is referred to as the intersection syndrome [Video 1] and [Figure 4C].

Overuse tenosynovitis of the abductor pollicis longus and extensor pollicis brevis tendons in the first extensor compartment (EC) is termed as De Quervain's tenosynovitis. It causes pain around the radial styloid associated with the movement of the thumb. The clinical diagnosis of de Quervain's tenosynovitis is usually straightforward using Finkelstein's test. Ultrasound [Figure 5A-G] is used to confirm the diagnosis, exclude underlying tendinosis or tendon tear, assess the retinaculum, detect whether septa are present within the first extensor compartment, and guide steroid injection [Video 2] into the tendon sheath or retinacular division in resistant cases. The APL or less commonly EPB tendon may have multiple tendon slips [Figure 5H], which should not be mistaken for longitudinal tendon clefts or tears.[2] The appearance of multiple tendon slips has been termed "the lotus root sign" because the multiple tendons appear similar to a cut lotus root.[3]

Acute tendon injuries tend to take the form of direct impact injury, stretch injury during contraction (strain), or penetrating injury. Depending on the site of tear of the tendon, injuries are classified into zones [Table 1]. The treatment and functional outcome depend on the zone of injury.[4,5] Ultrasound is useful to confirm the presence of tendon rupture [Figures 6 and 7], differentiate between the partial thickness and full thickness tears [Video 3], identify if the tear is associated with bony avulsion [Figure 8A-C], as well as to identify the precise location of the tendon ends.

In tendinosis, there is intratendinous mucinous degeneration with the tendon appearing hypoechoic and swollen without disruption of tendon fibers typically occurring because of overuse. Tendinosis may progress to partial-thickness and full-thickness tendon tear.

Calcific tendinitis of APB [Figure 9] is a rare entity[6] with patients presenting with pain along the radial aspect of the metacarpophalangeal joint. Ultrasound features of calcific tendinitis are thickening of the tendon, hyperechoic calcific foci and increased flow on color Doppler. Ultrasound guided steroid injection with needle decompression can be used to treat calcific tendinitis [Video 4].

Inflammation of the tendon sheath, called tenosynovitis, is common in patients with inflammatory arthritis. Ultrasound features of tenosynovitis are hypoechoic fluid in the tendon sheath, hyperemia on color or power Doppler (indicating active inflammation), and synovial hypertrophy with or without hypervascularization (indicating chronic disease). Fluid secondary to inflammation may accumulate proximal and distal to retinacula (for the extensor tendons) [Figure 10A and B] and pulleys (for flexor tendons) producing a lobulated appearance. Soft tissue thickening secondary to inflammation can also develop and surround the tendon [Figure 10C and D].

Trigger thumb is a transient locking of the thumb in flexion, followed by a painful snapping sensation during

extension. This occurs due to stenosing tenosynovitis at the level of the pulley (most common A1). Ultrasound [Figure 11] shows a thickened pulley, local swelling of the flexor tendons distal to the pulley, distal tenosynovitis, and small cysts at the pulley boundaries due to fluid trapping. In severe cases, dynamic scanning during passive flexion and extension shows difficult tendon gliding underneath the abnormal pulley [Video 5]. Doppler imaging may depict a hypervascular pattern in the pulley with surrounding soft tissues.[7] It is unclear if thickening of the A1 pulley initiates the blockage and tendon inflammation or if the thickening is secondary to tendinopathy.[8] Treatment is often corticosteroid injection near the level of the pulley or in the tendon sheath[9] and can be performed under ultrasound guidance. Failed conservative management may require surgical release.[10] Ultrasound-guided release using a bent 19 or 25 G hypodermic needle has been described.[11]

Table 1: Zones of flexor pollicis longus and extensor pollicis longus Tendon Injuries

Zones of FPL tendon injuries	
Zone I	Disruption of tendon insertion over base of distal phalanx
Zone II	Disruption of tendon over between neck of proximal phalanx and neck of metacarpal
Zone III	Disruption over thenar muscles
Zone IV	Disruption within carpal tunnel
Zone V	Disruption proximal to carpal tunnel
Zones of EPL tendon injuries	
Zone I	Disruption of terminal extensor tendon distal to or at IP joint of the thumb (EPL) Mallet Thumb
Zone II	Disruption of tendon over proximal phalanx of thumb
Zone III	Disruption over MCP joint of thumb (EPL and EPB
Zone IV	Disruption over the metacarpal of thumb (EPL and EPB)
Zone V	Disruption over CMC joint of thumb (EPL and EPB)

FPL: Flexor pollicis longus, EPL: Extensor pollicis longus

Evaluation of the nerves and vessels

Placing the probe in the transverse plane over the first compartment dorsally can identify radial artery and radial nerve. The radial artery is identified along the volar aspect of the tendons and the nerve is located superficial. On moving the probe distally, radial nerve and its branches can be seen crossing over from ventral to dorsal over the APL and EPB.

The Wartenberg syndrome occurs due to damage to the superficial branch of the radial nerve in the distal forearm/dorsal aspect [Figure 12] as a result of penetrating trauma, a tight watch-strap or iatrogenically (e.g. due to cephalic vein cannulation or retinaculum release in de Quervain disease). This can give rise to pain, paresthesia, and numbness over the dorsum of the hand and thumb.

Radial and Posterior interosseous nerve compression neuropathy [Figure 13] at the level of elbow and forearm can lead to weakness of EPL, EPB, and APL, with patients not being able to extend the thumb. Carpal tunnel syndrome and other pathologies of the median nerve at the level of the wrist, which can result in symptoms of the thumb, is a vast topic and are beyond the scope of this article.

Evaluation of collateral ligaments

To examine the Ulnar Collateral L igament (UCL), place the hand in a semipronated position [Figure 14A and B]. Coronal images are obtained by placing the probe at the long-axis of the thumb along the medial aspect of the first metacarpophalengeal joint. The examiner gives support and pressure from under the base of the thumb. Transverse images can be obtained by rotating the probe by 90°. Valgus stress views [Video 6] are taken in order to assess joint

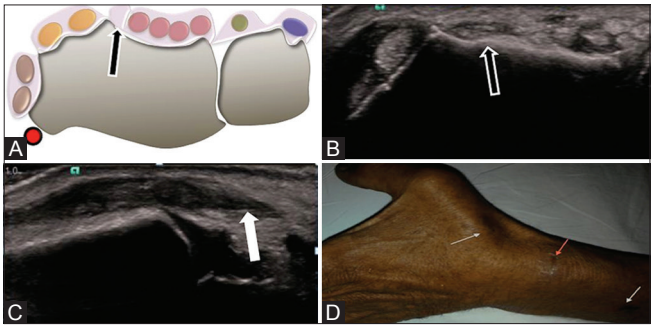

Figure 6 (A-D): Extensor pollicis longus tear (A-D). Schematic diagram (A) and short axis (B) ultrasound at the level of the wrist shows nonvisualization of the extensor pollicis longus tendon (black arrow) with only the tendon sheath remaining. Long axis (C) ultrasound shows the torn distal edge of the retracted extensor pollicis longus tendon (arrow). Patient photograph (D) with the site of incision and torn retracted edges marked with small white arrows

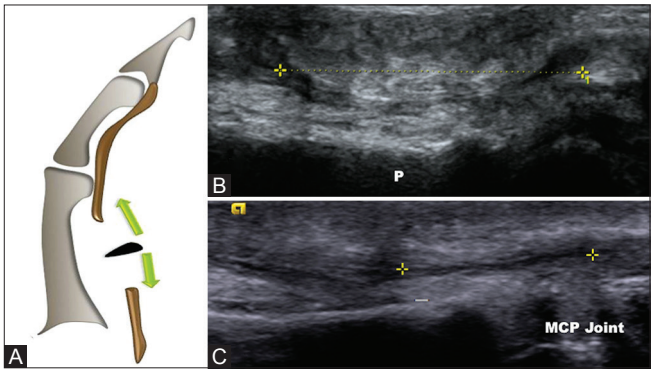

Figure 7 (A-C): Flexor pollicis longus tendon tear (A-C). Schematic diagram (A) shows tear of the flexor pollicis longus tendon with torn retracted edges. Long axis (B and C) ultrasound views in 2 different patients shows tear of the flexor pollicis longus tendon with retracted ends marked with calipers at different levels. (Proximal phalynx - P)

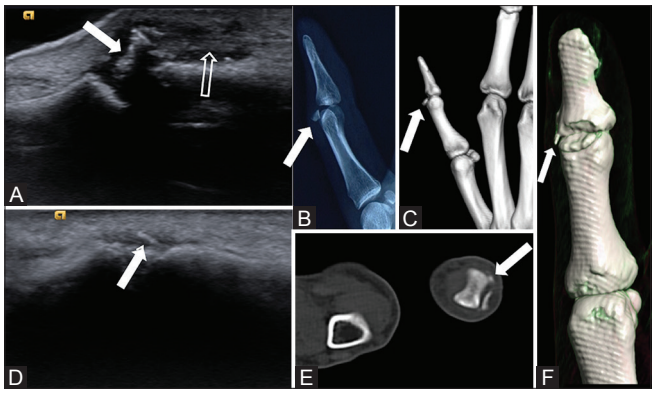

Figure 8 (A-F): Avulsed extensor pollicis longus (EPL) at insertion/mallet thumb (A-C) along with interphalengeal joint radial collateral ligament avulsion (D-F). Long axis (A) ultrasound shows an avulsed bony fragment from the dorsal aspect of the base of distal phalanx (arrow) with EPL tendon attached to it (open arrow). Lateral radiograph (B) and three-dimensional computed tomography–volume rendering technique image (C) of the thumb shows avulsed bony fragment. Long axis (D) ultrasound view along the lateral aspect of the interphalengeal joint shows thickened RCL with avulsed bony fragment. Axial CT (E) and three-dimensional volume rendering technique image (F) shows the avulsed bony fragment

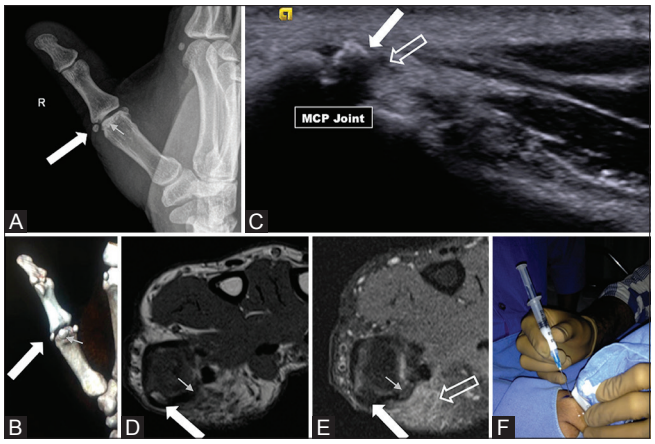

Figure 9 (A-F): A 55-year-old male with painful thumb abduction (A-F). Oblique radiograph (A) and reconstructed computed tomography–volume rendering technique image (B) of the thumb reveals subtle calcification along the lateral aspect of the base of proximal phalanx (arrow). Long axis (C) ultrasound of the thumb shows calcification (arrow) with heterogeneous hypoechoic area (open arrow) near the insertion of APB tendon. Axial T1 (D) and STIR (E) Magnetic resonance images of the thumb show calcification (arrow) and edema (open arrow) within the APB tendon/muscle. Steroid was injected using ultrasound guidance (F). Sesamoid bone (grey arrow)

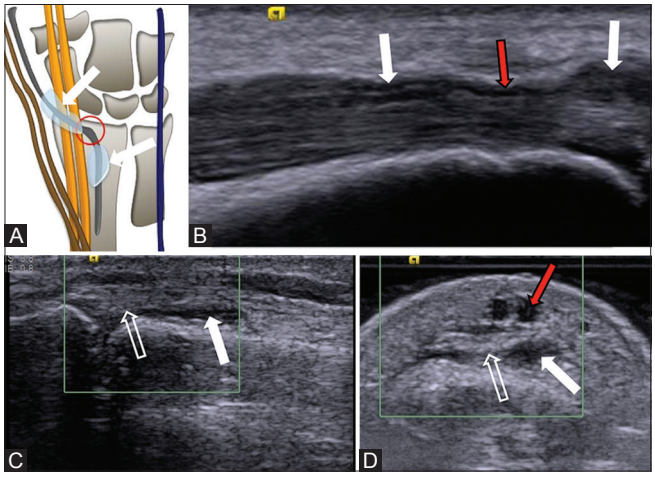

Figure 10 (A-D): EPL tenosynovitis (A-D). Schematic diagram (A) of the extensor tendons of the wrist shows the common site of EPL tendinopathy (represented in red circle). Long axis (B) ultrasound at the level of the wrist shows fluid around the extensor pollicis longus (EPL) tendon (white arrows) with absence of fluid at the level of retinaculum (red arrow). Short (C) and long (D) axis ultrasound at interphalengeal joint level shows soft tissue thickening (arrow) around the EPL tendon (open arrow). Subcutaneous veins are normally seen over the extensor tendon (red arrow in d) and should not be confused with tenosynovial fluid

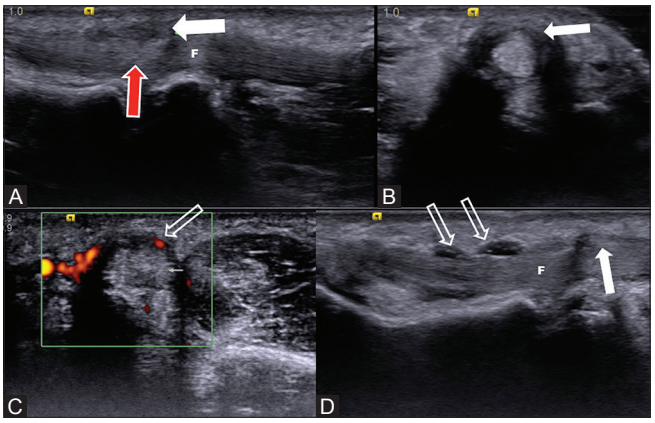

Figure 11 (A-D): Stenosing tenosynovitis of FPL tendon/trigger thumb (A-D). Long (A) and short (B and C) axis ultrasound images along the volar aspect of the thumb showing thickened A1 pulley of the thumb (white arrow) with increased vascularity (open arrow) within the thickened pulley and tendon thickening (red arrow). Long axis ultrasound image (D) along the volar aspect of the thumb shows ganglion cysts (open arrow) in the volar aspect of the flexor pollicis longus tendon along with thickened A1 pulley (white arrow). (FPL - F)

widening, compared with contralateral side. Stress testing is used to differentiate the torn ligament from an old scarred reattached ligament. The normal UCL [Figure 14B] is a hyperechoic structure spanning the ulnar side of the first metacarpophalangeal joint. Its configuration predisposes the deep fibers to anisotropy. Superficially, it is covered by an additional thin hyperechoic band corresponding to the adductor pollicis aponeurosis, which is variably visualized in the normal situation.[12] Gentle flexion of the metacarpophalan joints can be used to identify movement in the adductor aponeurosis. Similarly, the radial collateral ligament (RCL) can be evaluated [Figure 14C and D] by supinating the hand and placing the probe along the radial aspect of the first metacarpophalangeal joint.

Ulnar collateral ligament injury is graded into sprain, partial tear, and full thickness tear, and is referred to as the gamekeeper's thumb or skier's thumb.[13] Sprained ligaments appear thickened and hypoechoic owing to

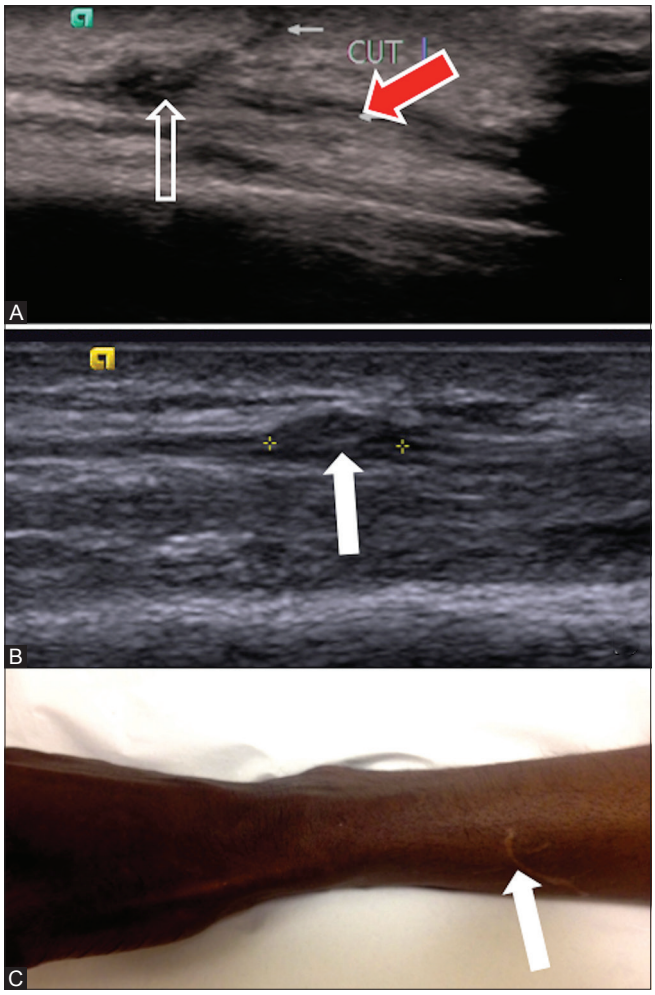

Figure 12 (A-C): Neuroma in the superficial branch of the radial nerve in a patient with cut injury presenting with pain and paresthesia over thumb (A-C). Long axis ultrasound view (A) of the superficial branch of the radial nerve (red arrow) with discontinuity (open arrow) and the cut site (small white arrow). Follow up long axis ultrasound (B) after 4 months shows neuroma formation (arrow). Patient photograph (C) shows the injury scar (arrow)

edema and hemorrhage, and appears as a thickened heterogeneous ligament with no disruption on dynamic valgus stress. The goal of imaging in tears of the UCL is to determine whether the torn ligament remains reduced [Figure 15A and B] [Video 7] or has displaced proximally. Visualization of an echogenic avulsion fracture fragment [Figure 15C-E] may be a clue to full-thickness tear. Absence of normal UCL fibers and presence of a heterogeneous mass proximal to the metacarpophalengeal joint is 100% accurate when diagnosing a complete UCL rupture.[14] UCL ligament tear can be associated with a Stener's lesion, which occurs when the torn UCL retracts proximally and folds on itself with the adductor aponeurosis interposed between the ruptured UCL and its site of insertion at the base of the proximal phalanx. The ultrasound appearance [Figure 16] of a Stener lesion has been likened to a yo-yo on

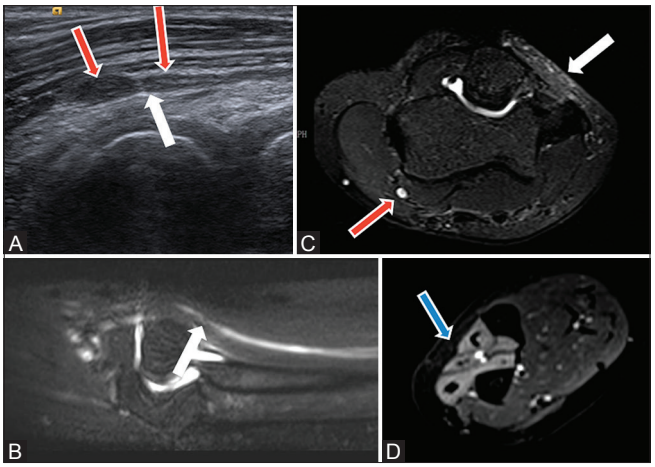

Figure 13 (A-D): Radial nerve compression neuropathy in a patient with inability to extend the thumb (A-D). Long axis ultrasound view (A) of the radial of nerve just proximal to the level of the elbow shows hour-glass configuration (white arrow) with proximal and distal nerve swelling (red arrows). magnetic resonance imaging shows narrowing of the radial nerve (white arrow) on an oblique three-dimensional STIR space sequence (B) with increased signal in the radial nerve (red arrow in C) on axial PD fat-sat image (C) and denervation edema within the extensor compartment muscles of the forearm (blue arrow in D) on axial STIR image (D)

a string, similar to findings on MRI. The string of the yo-yo represents the adductor pollicis aponeurosis, and the yo-yo represents the balled-up and displaced proximal portion of the ulnar collateral ligament. This precludes successful primary healing since the ruptured ends of the ligament are no longer in contact, resulting in long-term morbidity. Surgical repair is needed to avoid permanent instability and early osteoarthritis.[12]

Radial collateral ligament (RCL) is not a mirror image of its ulnar counterpart due to lack of aponeurosis [Figure 14D].[12] RCL tears are less common than the UCL tears and are associated with profound ulnovolar joint subluxation due to unopposed action of the adductor pollicis aponeurosis. The ultrasound appearances of tears are similar to those of UCL tears and can be associated with or without a bone avulsion. No Stener lesion is identified with RCL tears.

Evaluation of the pullies, volar plate, and sesamoid bones

The annular pulleys are best identified on long axis with dynamic movement of the flexor tendons. Place the probe over the metacarpophalengeal joint and interphalengeal joint and look for a thin hypo reflective band measuring no more than 5–6 mm in length and overlying the tendon just proximal to the level of the joint. Gentle finger movement will show the tendon moving independently of this structure.

A pulley tear of the thumb only rarely occurs in comparison to the fingers.[15] Ultrasound features of pulley injury include

abnormal hypoechogenicity or absence of the pulley. An important indirect sign of a pulley tear is abnormal volar displacement of the flexor tendons, called bowstringing, evaluated dynamically during active forced finger flexion.[16]

Volar/plamer plate complex consists of the volar plate, which can be identified by pacing the probe along the long- and short-axis over the metacarpophalengeal [Figure 1E] and interphalengeal joints [Figure 1I] and can be seen as echogenic areas [Figure 1G and K]. Sesamoid bones and the interconnecting intersesamoidal ligament that form a part of the volar plate complex (at the level of the metacarpophalengeal joint) are seen embedded within the volar plate with the FPL traversing in between. The volar plate complex can be injured [Figure 17] by forced hyperextension of the metacarpophalengeal joint either with or without a bony fracture on the volar aspect of the base of the proximal phalanx and can be associated with ulnar collateral ligament injury.

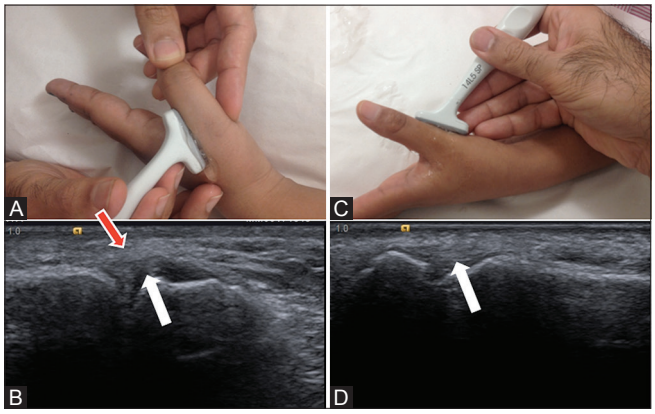

Figure 14 (A-D): Probe position and ultrasound images for evaluation of collateral ligaments metacarpophalengeal joint level (A-D). Probe position with hand in semipronation for UCL evaluation (A) with corresponding ultrasound image (B) shows the UCL (white arrow) and adductor aponeurosis (red arrow). Probe position with hand in semisupination for evaluation of the RCL (C) with corresponding ultrasound image (D) shows RCL (white arrow). (UCL - Ulnar collateral ligament, RCL - Radial collateral ligament)

Soft tissue tumors of the thumb

Ultrasound is the initial imaging modality of choice for tumor and tumor-like lesions of the thumb. Ultrasound can differentiate between a cystic versus a solid and hypovascular versus hypervascular lesions (using color Doppler). It can also assess the relationship between tendons and the mass lesions. The common tumors of the thumb include ganglion cysts arising from the joint or the flexor tendons, giant cell tumors of the tendon sheath, schwanoma/neurofibroma, glomus tumors, hemangiomas, and lipomas.

Ganglion cyst is a soft tissue lump that may occur in any joint, and most often occurs on, or around, near joints. Ganglion cysts most frequently arise from the dorsal aspect of the wrist, whereas those from the flexor tendons, usually arise near the A1 pulley [Figure 11D].[17] Ultrasound of a ganglion cyst shows a well-demarcated anechoic mass, with posterior acoustic enhancement, but appearances vary depending on size and chronicity.[18] Septa and hyperechoic

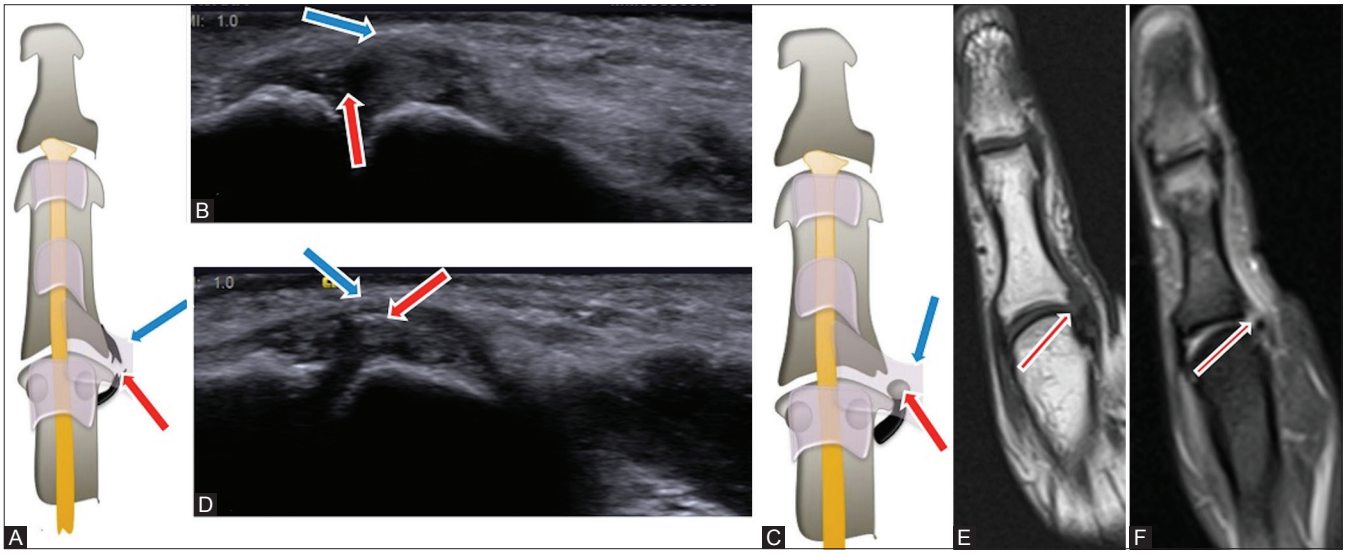

Figure 15 (A-F): Ulnar collateral ligament tear (A-B). Schematic diagram (A), long axis ultrasound (B) shows intrasubstance reduced tear of the UCL (red arrow) with normally positioned adductor pollicis aponeurosis (blue arrow). Schematic diagram (C) and long axis ultrasound (D) show avulsed UCL with bony fragment (red arrow) and normally positioned adductor pollicis aponeurosis (blue arrow). Magnetic resonance imaging show avulsed UCL (red arrow) on coronal T1 (E) and PD fat-sat (F) images. A small bony defect was noted along the inferomedial aspect of the base proximal phalanx

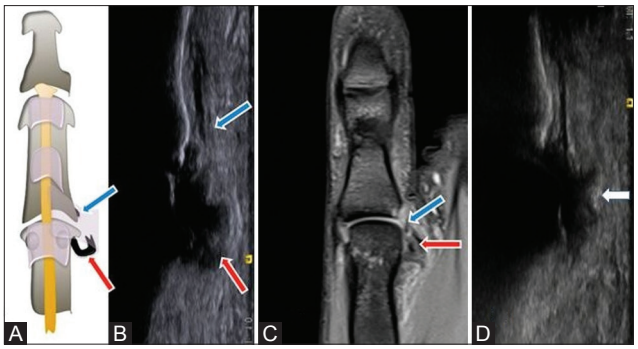

Figure 16 (A-D): Ulnar collateral ligament tear with Stener's lesion (A-D). Schematic diagram (A) and long axis ultrasound (B) and coronal PD fat sat MRI (C) shows torn proximally retracted balled-up ulnar collateral ligament (red arrow) with distally interposed adductor pollicis aponeurosis (blue arrow). Long axis ultrasound (D) in another patient shows ulnar collateral ligament tear with Stener's lesion with avulsed bony fragment (white arrow)

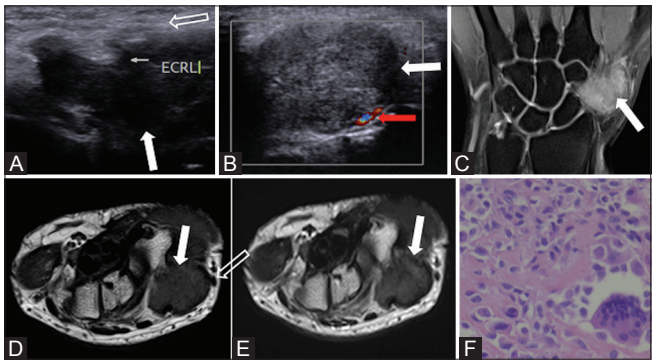

Figure 18 (A-F): Giant cell tumor (A-E). Long (A) and short (B) axis ultrasound images along the the dorsal aspect of the base of the thumb show a hypoechoic mass (white arrow) encasing the ECRL tendon with extensor pollicis longus tendon displaced (open arrow in A and D) and radial artery lying deep to the lesion (red arrow). Magnetic resonance imaging show a relatively well-defined lobulated mass lesion (white arrow) appearing hyperintense on coronal PD fat-sat images (C) and hypointense on both T1 (D) and T2 (E) weighted images. (F) H and E stain histopathological photomicrograph (×40)

contents are seen in older ganglia, which may not appear obviously cystic. Hypervascularity of a thickened wall may also be appreciated.[19] Ultrasound can be used to guide aspiration or steroid injection.

Giant cell tumors (GCT) of the tendon sheath appear as well-defined, hypoechoic masses, predominantly homogeneous, although heterogeneous lesions are described. Color or power Doppler imaging shows internal vascularity, peripheral or central, or a combination of the two. Although the ultrasound appearance [Figure 18] is not diagnostic, the proximity to the tendon sheath is highly suggestive of GCT of tendon sheath.[20]

Lipomas [Figure 19] are soft, painless, well-delineated, and mobile masses with variable echogenicity that

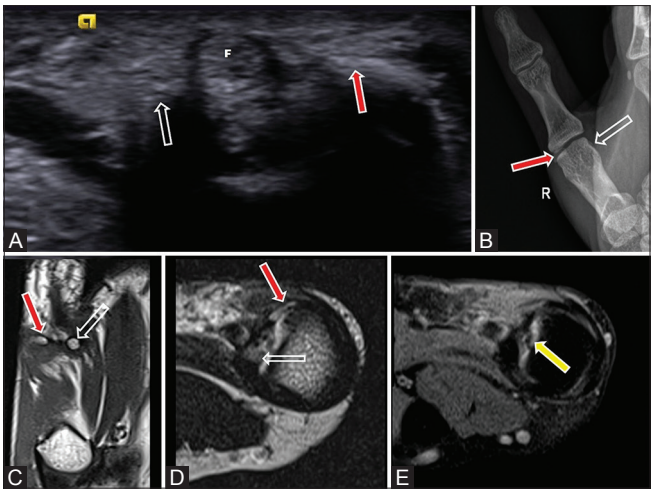

Figure 17 (A-E): Volar plate complex injury (A-E). Short axis ultrasound (A) and radiograph (B) shows obliquely rotated radial sesmoid (red arrow) with the normal ulnar sesmoid (open arrow). The radiograph also shows the radial sesmoid (red arrow) to be distally displaced at the level of the metacarpophalengeal joint. Magnetic resonance imaging shows the obliquely oriented radial sesmoid (red arrow) and normally oriented ulnar sesmoid (open arrow) on coronal T1 (C) and axial T2 (D) with increased signal in the volar plate and intersesmoidal ligament (yellow arrow) in axial PD fat sat image (E). (F - FPL, R - Right)

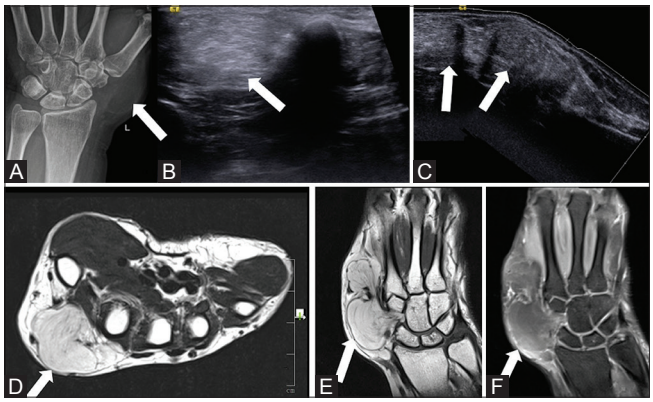

Figure 19 (A-F): Lipoma of thumb (A-F). Antero-posterior radiograph (A) of the wrist shows a radiolucent lesion along the lateral aspect of the thumb (arrow). Short axis (B) and panoramic (C) ultrasound images show the lesion to be hyperechoic (arrow). Magnetic resonance imaging shows the lesion (arrow) to be hyperintense on axial T2 and coronal T1 (E) images with complete suppression on PD fat suppressed image (F)

ranges from hypoechoic to hyperchoic, related to cellular variability.[21,22]

If ultrasound fails to provide an answer, MRI is an accurate problem solver for evaluating mass lesions, but is relatively infrequently needed.

Malignant tumors of the thumb are rare. Synovial sarcoma [Figure 20] arises in the periarticular location contrary to what its name suggests. Ultrasound features of synovial sarcomas can be variable ranging from homogenously hypoechoic lesions with well defined

margins to markedly heterogeneous lesions with ill-defined margins.[23]

Foreign body

Traditionally, plain radiographs have been the first modality of choice for the diagnosis of foreign bodies. However, non-radiopaque foreign bodies in the soft tissue are difficult to localize on radiographs. For detection of superficial, nonradiopaque foreign bodies, ultrasound has been shown to be more effective than even computed tomography.[24,25] Familiarity with the ultrasound appearances [Figure 21] of soft-tissue foreign bodies and a systematic evaluation of the region of interest in both the longitudinal and transverse orientations are needed for accurate assessment.

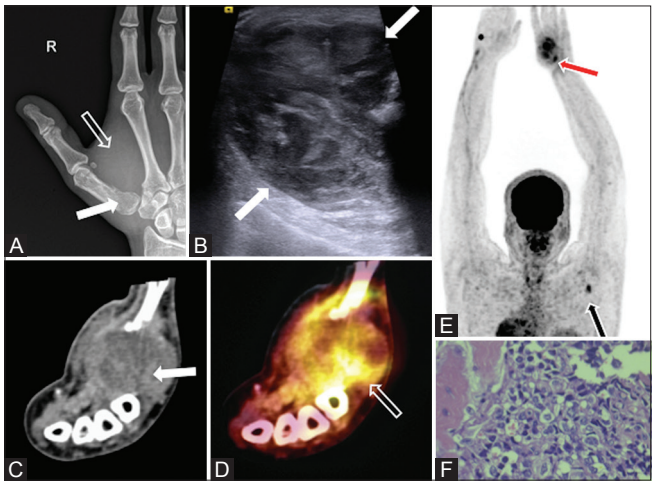

Figure 20 (A-F): Synovial sarcoma of the thumb (A-F). Antero-posterior radiograph (A) of the thumb shows destruction at the base of 1st metacarpal (arrow) with prominent adjoining soft tissue (open arrow). Short axis ultrasound image (B) of the thenar region shows a mixed echogenic lesion (arrow). CT (C) and fused FDG-18 PET-CT (D) images show the lesion to be heterogeneously enhancing with increased FDG-18 uptake (open arrow). Three-dimensional FDG-18 PET image (E) shows increased uptake in the thumb (red arrow) and in an axillary node (black arrow). (F) H and E stain histopathological photomicrograph (×40)

Conclusion

Musculoskeletal ultrasound is a user-dependent technique with a steep learning curve. Evaluation of various pathologies of the thumb pertaining to tendons, pulley, and collaterals are better assessed using ultrasound because of its high resolution, dynamic technique, and access to correlation with the opposite side. Certain pathologies such as soft tissue tumors may need MRI for tissue characterization and to assess the involvement of deeper structures for surgical planning. MRI may have an added advantage in evaluation of compressive neuropathies by detecting denervation muscular edema and identifying nerve edema. Ultrasound is also helpful in guiding interventions for various pathologies of the thumb.

Financial support and sponsorship

Nil.

Conflicts of interest

There are no conflicts of interest.

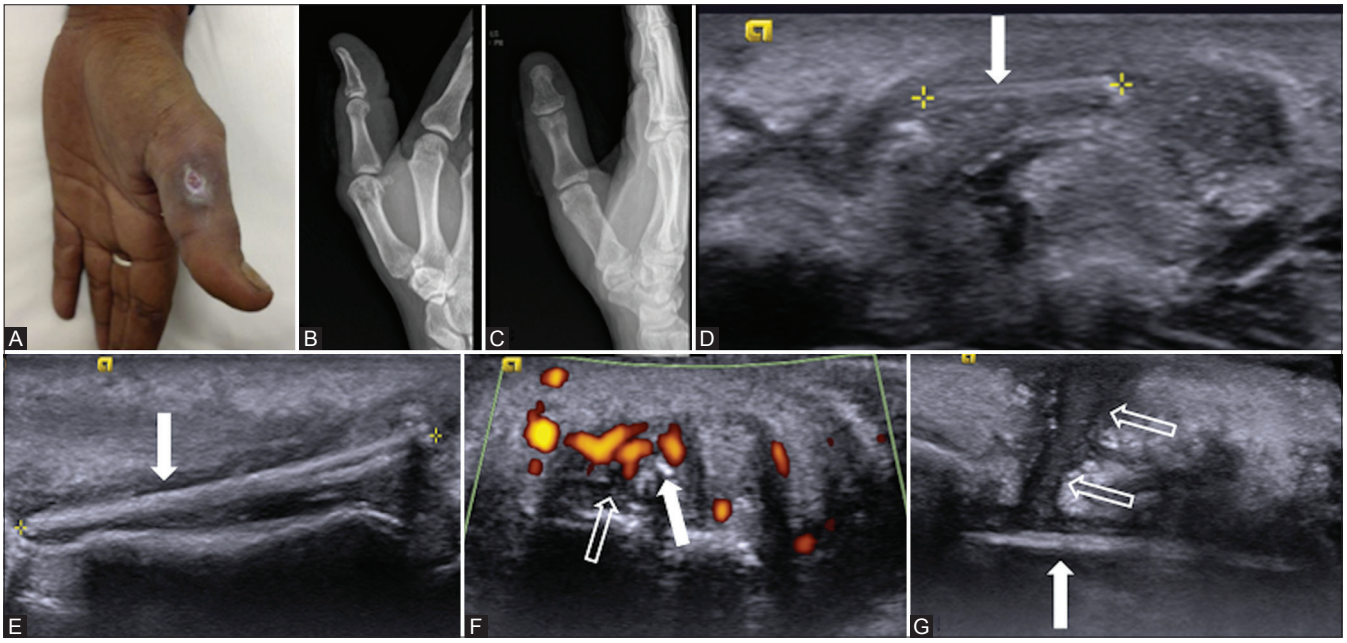

Figure 21 (A-G): Foreign body (thorn) in thumb (A-G). Patient photograph (A) shows the site of prick in the lateral aspect of the proximal thumb. Antero-posterior (B) and oblique (C) radiographs show the foreign body to be non-radio-opaque. Long (D and E) and short (F) axis ultrasound images show two hyperechoic foreign bodies (arrows) with surrounding hypervascular granulation tissue (open arrow in F). Long axis ultrasound (G) image shows granulation tissue/abscess (open arrow) tracking from the skin up to the foreign body (arrow)

References

1. Eaton RG, Glickel SZ. Trapeziometacarpal osteoarthritis: Staging as a rationale for treatment. Hand Clin 1987;3:455-71.
2. Rousset P, Vuillemin-Bodaghi V, Laredo JD, Parlier-Cuau C. Anatomic variations in the first extensor compartment of the wrist: Accuracy of US. Radiology 2010;257:427-33.
3. Choi SJ, Ahn JH, Lee YJ, Ryu DS, Lee JH, Jung SM, *et al*. de Quervain disease: US identification of anatomic variations in the first extensor compartment with an emphasis on subcompartmentalization. Radiology 2011;260:480-6.
4. Griffin M, Hindocha S, Jordan D, Saleh M, Khan W. An Overview of the management of flexor tendon injuries. Open Orthop J 2012;6:28-35.
5. Griffin M, Hindocha S, Jordan D, Saleh M, Khan W. Management of Extensor Tendon Injuries. Open Orthop J 2012;6:36-42.
6. Shields JS, Chhabra AB, Pannunzio ME. Acute calcific tendinitis of the hand: 2 case reports involving the abductor pollicis brevis. Am J Orthop 2007;36:605-7.
7. Guerini H, Pessis E, Theumann N, Le Quintrec JS, Campagna R, Chevrot A, *et al*. Sonographic appearance of trigger fingers. J Ultrasound Med 2008;27:1407-13.
8. Serafini G, Derchi LE, Quadri P, Martinoli C, Orio O, Cavallo A, *et al*. High resolution sonography of the flexor tendons in trigger fingers. J Ultrasound Med 1996;15:213-9.
9. Peters-Veluthamaningal C, van der Windt DA, Winters JC, Meyboom-de Jong B. Corticosteroid injection for trigger finger in adults. Cochrane Database Sys Rev 2009:CD005617.
10. Benson LS, Ptaszek AJ. Injection versus surgery in the treatment of trigger finger. J Hand Surg Am 1997;22:138-44.
11. Rajeswaran G, Lee JC, Eckersley R, Katsarma E, Healy JC. Ultrasound-guided percutaneous release of the annular pulley in trigger digit. Eur Radiol 2009;19:2232-7.
12. Ebrahim FS, De Maeseneer M, Jager T, Marcelis S, Jamadar DA, Jacobson JA. US diagnosis of UCL tears of the thumb and Stener lesions: Technique, pattern-based approach, and differential diagnosis. Radiographics 2006;26:1007-20.
13. Hergan K, Mittler C, Oser W. Pitfalls in sonography of the gamekeepers' thumb. Eur Radiol 1997;7:65-9.
14. Melville D, Jacobson JA, Haase S, Brandon C, Brigido MK, Fessell D. Ultrasound of displaced ulnar collateral ligament tears of the thumb: The Stener lesion revisited. Skeletal Radiol 2013;42:667-73.
15. Kosiyatrakul A, Jitprapaikulsarn S, Durand S, Oberlin C. Closed flexor pulley rupture of the thumb: Case report and review of literature. Hand Surg 2009;14:139-42.
16. Bayat A, Shaaban H, Giakas G, Lees VC. The pulley system of the thumb: Anatomic and biomechanical study. J Hand Surg Am 2002;27:628-35.
17. Bianchi S, Della Santa D, Glauser T, Beaulieu JY, van Aaken J. Sonography of masses of the wrist and hand. AJR Am J Roentgenol 2008;191:1767-75.
18. Teefey SA, Dahiya N, Middleton WD, Gelberman RH, Boyer MI. Ganglia of the hand and wrist: A sonographic analysis. AJR Am J Roentgenol 2008;191:716-20.
19. Wang G, Jacobson JA, Feng FY, Girish G, Caoili EM, Brandon C. Sonography of wrist ganglion cysts: Variable and noncystic appearances. J Ultrasound Med 2007;26:1323-8.
20. Middleton WD, Patel V, Teefey SA, Boyer MI. Giant cell tumors of the tendon sheath: Analysis of sonographic findings. AJR Am J Roentgenol 2004;183:337-9.
21. Fornage BD, Tassin GB. Sonographic appearances of superficial soft tissue lipomas. J Clin Ultrasound 1991;19:215-20.
22. Inampudi P, Jacobson JA, Fessell DP, Carlos RC, Patel SV, Delaney-Sathy LO, *et al*. Soft-tissue lipomas: Accuracy of sonography in diagnosis with pathologic correlation. Radiology 2004;233:763-7.
23. Marzano L, Failoni S, Gallazzi M, Garbagna P. The role of diagnostic imaging in synovial sarcoma: Our experience. Radiol Med 2004;107:533-40.
24. Boyse TD, Fessell DP, Jacobson JA, Lin J, van Holsbeeck MT, Hayes CW. US of soft-tissue foreign bodies and associated complications with surgical correlation Radiographics 2001;21:1251-6.
25. Tahmasebi M, Zareizadeh H, Motamedfar A. Accuracy of ultrasonography in detecting radiolucent soft-tissue foreign bodies. Indian J Radiol Imaging 2014;24:196-200.